Clim. Past Discuss., 9, 4263–4291, 2013
www.clim-past-discuss.net/9/4263/2013/
doi:10.5194/cpd-9-4263-2013

Climate of the Past
Discussions
Open Access

Proof in climatology for circulation effect of stalagmite δ^{18}O in East Asia: analysis on the ratios among water vapor transport passageway intensities in East Asia

S. Nan[1], M. Tan[2], and P. Zhao[1]

[1]Chinese Academy of Meteorological Sciences, Beijing 100081, China
[2]Key Laboratory of Cenozoic Geology and Environment, institute of Geology and Geophysics, Chinese Academy of Sciences, Beijing 100029, China

Received: 8 June 2013 – Accepted: 15 July 2013 – Published: 29 July 2013

Correspondence to: S. Nan (nansl@cams.cma.gov.cn)

Published by Copernicus Publications on behalf of the European Geosciences Union.

Abstract

Further verification about the circulation effect of stalagmite $\delta^{18}O$ in East Asian monsoon region needs the quantitative description for the proportion of water vapor transport (WVT) from different source regions. WVT passageway intensities are defined as regionally averaged WVT flux modes in this paper. The ratio between two WVT passageways' intensities represents relative intensity of the two WVT passageways. Using the NCEP-NCAR reanalysis data for 1948–2011, the ratios of the intensities of three WVT passageways from low latitudes (the intensity of WVT from Bay of Bengal (IBOB), the intensity of WVT from South China Sea (ISCS) and the intensity of WVT from western North Pacific (IWNP) in summer are calculated. SB is for the ISCS-IBOB ratio, WB for the IWNP-IBOB ratio, and WS for the IWNP-ISCS ratio. The decadal increase occurs in the time series of WB and WS, with higher values in 1976–1995 and lower values in 1950–1975, probably resulting from the strengthening of WVT from WNP in the midterm of 1970s. East Asian atmospheric circulations, WVTs and previous SST characters corresponding to the ratios are analyzed. The result indicates that SB, WB and WS may properly reflect the relative intensities between ISCS and IBOB, between IWNP and IBOB, and between IWNP and ISCS, respectively. For high SB years, the Asian Low and the western Pacific subtropical high (WPSH) weaken. The southwesterly winds from BOB to the Yangtze River valley by the southeast of the Tibetan Plateau weaken and the WVT from BOB to East Asia weakens. The southwesterly winds from SCS to East Asia strengthen and the WVT from SCS to East Asia strengthens. In high WB years, the Asian Low weakens and the WPSH shifts westwards, enhances and enlarges. The WVT from WNP to East Asia increases because of the strengthening of the easterly winds on the south of the WPSH. The westerly winds from BOB to East Asia by Indo-China Peninsula decrease and the WVT from BOB to East Asia weakens. The atmospheric circulation and WVT associated with WS are similar with those associated with WB. There are close relationships between WB (and WS) and the WPSH area, position and intensity. In high WB (and WS) years, the WPSH shifts westwards,

CPD

9, 4263–4291, 2013

enlarges and enhances. There is no obvious anomalous previous SST signal in tropical Indian Ocean and equatorial central and eastern Pacific for anomalous SB years. WB and WS are closely related to previous SST signal. When the equatorial central and eastern Pacific is in El Niño phase, SST in the tropical Indian Ocean, BOB and SCS is high and SST at middle latitudes in North Pacific is low, WB and WS tend to be high. After the midterm of 1970s, the equatorial central and eastern Pacific is often in El Niño phase. It is in agreement with higher WB in 1976–1995 than that in 1950–1975. In light of circulation effect of stalagmite δ^{18}O in East Asia, high WB implies high stalagmite δ^{18}O. Therefore, the interdecadal increase of WB in 1976–1995 than in 1950–1975 provides the proof using the conception of circulation effect to explain the interdecadal change of stalagmite δ^{18}O at most regions in East Asia.

1 Introduction

Absolutely-dated oxygen isotope records from Chinese stalagmites have supplied chronologic benchmark for late Pleistocene paleoclimate research (e.g. Wang et al., 2001, 2008; Yuan et al., 2004; Cheng et al., 2009), meanwhile aroused great debate worldwide over the past few years due to a lack of quantitative calibration (e.g. Maher, 2008, 2012; Dayem et al., 2010; Clemens et al., 2010; Pausata et al., 2011; Lee et al., 2012). In view of this, it may be worth considering comparing the stalagmite δ^{18}O records ($\delta^{18}O_s$) formed during the observation period with meteorological data.

So far, we could get eight published $\delta^{18}O_s$ series from Chinese caves which span the period of 1950's to now from NOAA website (http://www.ncdc.noaa.gov/paleo/speleothem.html). In the order from north to south, the $\delta^{18}O_s$ are from Shihua Cave in Beijing, Wanxiang and Huangye Cave in Gansu, Dayu Cave in Shanxi, Heshang Cave in Hubei, Lianhua Cave in Hunan and Dongge Cave in Guizhou, respectively (see Supplement Fig. S1). The distinctive feature herein is that all of the $\delta^{18}O_s$ show higher values in 1976–1995 than those in 1950–1975 except the record from Lianhua Cave which is obviously heavier than other records. Precipitation in China, as we have

CPD
9, 4263–4291, 2013

known, is not reduced synchronously from north to south from 1950–1975 to 1976–1995. Therefore, amount effect is not responsible for this situation. What caused the decadal shift? Tan (2009) present a concept "circulation effect" to interpret the short-term change in the $\delta^{18}O_s$ in East Asia. Then, the subsequent question is presented: could the "circulation effect" explain the decadal shift in the $\delta^{18}O_s$ in East Asia from 1950–1975 to 1976–1995? The "circulation effect" is referred that the changes in $\delta^{18}O_s$ in East Asia could reflect the variable ratio of the remote water vapor from the Indian Ocean and the local water vapor from the Pacific caused by the variability of large-scale atmospheric-oceanic circulation. Later, Tan (2013) further points out that the southwest monsoon drives long distance water vapor transport (WVT) from Indian Ocean to the East Asia, and along this pathway increasing rainout leads to more negative $\delta^{18}O$ via Rayleigh distillation processes. In contrast, the southeast monsoon, which closely related with the changes in the strength of the western Pacific subtropical high (WPSH), drives short-distance WVT from the western North Pacific to East Asia and leads to less negative $\delta^{18}O$. Thus, to quantitatively describe the relative intensity of the remote and local WVTs becomes necessary.

The WVT is one of the most important components of the East Asian monsoon system. A large amount of water vapor is directly carried from the adjacent oceans to East Asia (Lau and Li, 1984; Tao and Chen, 1987; Jiang and Li, 2009). There are four WVT passageways directly entering into East Asian continent in summer: (1) the southwesterly monsoon in South China Sea (SCS) transports the water vapor to East Asian continent; (2) the southeasterly air current on the west and southwest of the WPSH transports the water vapor from the western Pacific to East Asian continent; (3) the southwesterly summer monsoon directly transports the water vapor from Bay of Bengal (BOB) to East Asian continent; (4) the westerly wind at the mid-high latitudes transports the water vapor to East Asian continent. Among the four WVT passageways, the WVT from the westerly wind at the mid-high latitudes is the lowest. Other three passageways' water vapor comes from oceans at low latitudes.

CPD
9, 4263–4291, 2013

In the past research on the WVTs in East Asia from climatologists, the WVTs are referred as a part of Asian monsoon system and closely related with atmospheric circulations and monsoon precipitation. The summer rain belts in China are closely associated with the WVT passageways and sources. Simmonds et al. (1999) investigate the summer WVT by the large-scale circulation over China and conclude that the WVT that supports the summer rainfall over southeast China comes mainly from the SCS and the western Pacific and the Indian monsoon circulation plays little part in determining the character of the differences between the wet and dry years. Xie et al. (2002) indicate that when the precipitation in the mid-lower reaches of the Yangtze River valley is heavy, the WVT tends to be strong and stable, deriving from BOB, passing by the southern China and arriving at the western Pacific. Meanwhile, the WVT is often weak, deriving from BOB, passing by the Indo-China Peninsula and arriving at the SCS. Tian et al. (2002) indicate that the more precipitation in North China corresponds to the anomalous southwesterly WVT on the northwest of the WPSH. Zhou and Yu (2005) indicate that the tropical WVT for a heavier rain belt along the mid-lower reaches of the Yangtze River valley comes directly from BOB and SCS, and the subtropical branch for a main rain belt along the Huaihe River valley comes directly from SCS. Zhuo et al. (2006) present that for the drought years in Yangtze and Huaihe River basins, the WVT on the west borderline of the China continent is obviously less than that for the flood years. These studies provide the theoretical basis to calculate the relative intensity of the remote and local WVTs.

The main objective of this paper is to reveal the relative intensity of the remote and local WVTs in East Asia and the associated features of the atmospheric circulation, WVT and previous SST signal. Based on the analysis, we will further demonstrate the important role of the intensities of the WVT passageways in using the circulation effect to explain the decadal variability of $\delta^{18}O_s$ from 1950–1975 to 1976–1995 in East Asia. The paper is organized as follows. In Sect. 2, the data and calculation are described. The relative intensities of the WVT passageways are calculated in Sect. 3. The atmospheric circulations and the WVTs associated with the relative intensities of the WVT

CPD
9, 4263–4291, 2013

passageways are shown in Sect. 4. The SST variation associated with the relative intensities of the WVT passageways is described in Sect. 5. Discussion and conclusions of this study follow in Sect. 6.

2 Data and calculation

Global reanalysis data sets provided by NCEP-NCAR for the period 1948–2011 are used to calculate the terms of the atmospheric WVT (Kalnay et al., 1996). The physical variables used in this study include the monthly specific humidity, and the meridional and zonal wind components at eight standard pressure levels, namely, 1000, 925, 850, 700, 600, 500, 400, and 300 hPa. The geopotential heights at 850 hPa and 500 hPa are used to describe the atmospheric circulation variation. The surface pressure is used to treat the impact of topography. The monthly mean SST from the HadISST data set for the period of 1947–2011 is used in this study (Rayner et al., 2003). The NCEP-NCAR and HadISST data have horizontal resolutions of 2.5° and 1°, respectively. The vertically integrated moisture flux can be expressed as

$$\boldsymbol{Q} = \frac{1}{g}\int_{p_t}^{p_s} \boldsymbol{V} q \, \mathrm{d}p \tag{1}$$

where $\boldsymbol{V}$ is the horizontal wind vector, q is specific humidity, p_s is the lower boundary (here, the surface pressure), p_t is the upper boundary (here, 300 hPa), p is the pressure, and g is the acceleration due to gravity. Since the NCEP-NCAR reanalysis sets the specific humidity to zero above 300 hPa, the vertical integration of Eq. (1) is performed from the surface to 300 hPa. The missing data above 300 hPa has a nearly negligible impact on the result because of the concentration of water vapor in the lower troposphere (Zhou, 2003).

CPD
9, 4263–4291, 2013

3 The rations of the intensities of the WVT passageways (RIWVTPs)

3.1 The intensity of WVT passageways

Now, we review the summer moisture transport in East Asia and associated atmospheric circulation systems. Figure 1 is the climatological mean WVT flux vectors vertically integrated in summer for the period 1948–2011. There are three branches of WVTs from the oceans at low latitudes to East Asia. The first is the southwesterly monsoon (Indian monsoon) transport, deriving from South Indian Ocean, crossing the equator in Somali, and passing by the Arabian Sea, the BOB (a part directly enters into China), Indo-China Peninsula and SCS into the eastern China. The second is the Asian–Australian monsoon transport, which crosses the equator and converges with the flow of the Indian monsoon at SCS into China. The third is southeasterly monsoon transport on the west and southwest of the WPSH. Because of the guide of the WPSH, the robust moisture arrives at the eastern China from the western Pacific. The oceanic regions which directly transport the water vapor to East Asia are BOB, SCS and WNP. The regionally-averaged moisture flux modes are defined to represent the intensities of the WVT passageways: the intensity of WVT passageway from WNP (125–150° E; 10–22.5° N, IWNP), the intensity of WVT passageway from SCS (107.5–120° E; 10–22.5° N, ISCS), and the intensity of WVT passageway from BOB (85–100° E; 10–22.5° N, IBOB). The selected regions are in accord with those selected by Tian et al. (2004).

3.2 Time series for the intensity of WVT passageways

Figure 2 shows the time series of the intensities of the three WVT passageways. The three intensities all show the obvious interannual variations. IWNP is higher in 1976–1995 than in 1950–1975. Later, we will indicate the decadal shift is closely related with that of the $\delta^{18}O_s$ in East Asia. Based on the circulation effect of the $\delta^{18}O_s$ in East Asia (Tan, 2009, 2013), the WVT from WNP is local source and its increase helps the $\delta^{18}O_s$

CPD
9, 4263–4291, 2013

to get heavier. IBOB shows the decreasing trend from 1948 to now. In climatology, IBOB is the strongest with the mean value of 3400 $g\,cm^{-1}\,hPa^{-1}\,s^{-1}$ for the period 1948–2011 and ISCS is slightly stronger than IWNP (Table 1). For the standard deviations, IBOB has the widest amplitude and ISCS has the slightly wider amplitude than IWNP (Table 1). The mutual-correlation analyses show the weak correlations between IBOB and IWNP and between ISCS and IWNP, implying the independence between IBOB and IWNP and between ISCS and IWNP. There is significant correlation between IBOB and ISCS (their correlation coefficient is 0.61), due to the flow in SCS including the part of the easterly transport of southwesterly monsoon from BOB.

3.3 Time series for the RIWVTPs

The RIWVTPs are calculated with the WVT passageways' intensities. SB is for the ISCS-IBOB ratio, WB for the IWNP-IBOB ratio, and WS for the IWNP-ISCS ratio. SB, WB and WS reflect the relative intensities among the three WVT passageways. High SB values mean the WVT from SCS is stronger than normal relative to that from BOB. High WB values mean the WVT from WNP is stronger than normal relative to that from BOB. High WS values mean the WVT from WNP is stronger than normal relative to that from SCS. Figure 3 indicates the time series of SB, WB and WS for the period 1948–2011. They all present the obviously interannual variation. Both WB and WS show the decadal increase from 1950–1975 to 1976–1995, probably resulting from the decadal increase of IWNP. In light of the circulation effect (Tan, 2009, 2013), the $\delta^{18}O_s$ in East Asia is controlled by the ratio of the local and remote WVTs. For East Asia, WMP is local and BOB is remote. The increase of WB means the increase of the local and remote moisture proportion, resulting in the increase of the stalagmite $\delta^{18}O$ in East Asia.

4 Atmospheric circulations and WVTs associated with the RIWVTPs

SB, WB and WS are defined and expected to reflect the relative intensities of different WVT passageways. Do they properly reflect the relative intensities? To detect the atmospheric circulations and WVTs associated with SB, WB and WS, we select 10 high and low SB, WB and WS years to conduct the composite analysis. They are 1950, 1951, 1954, 1972, 1975, 1985, 1997, 1998, 2002 and 2005 for high SB years and 1949, 1956, 1962, 1969, 1970, 1971, 1980, 1982, 1989 and 2011 for low SB years. The 10 high WB years are 1965, 1983, 1986, 1992, 1995, 1998, 2000, 2003, 2004 and 2010 and the 10 low WB years are 1959, 1961, 1962, 1963, 1967, 1968, 1971, 1982, 1994 and 2008. The 10 high WS years are 1980, 1983, 1986, 1987, 1992, 1995, 2003, 2004, 2010 and 2011 and the 10 low WS years are 1950, 1959, 1961, 1967, 1968, 1972, 1984, 1985, 1994 and 1997. The years are selected based on the time series of SB, WB and WS, which show the interannual-decadal variations. Therefore, the results reflect the interannual-decadal features of atmospheric circulations and WVTs associated with SB, WB and WS.

Figure 4a is the composite difference of 850 hPa geopotential height between the high and low SB years. The Asian continent is covered by positive values, indicating the weakened Asian Low. The negative values appear over the western North Pacific, indicating the weakened WPSH. In 850 hPa horizontal winds (Fig. 5a), an anomalous anti-cyclonic circulation appears over BOB and Indian subcontinent and an anomalous cyclonic circulation appears over the western Pacific, SCS and the eastern China. Between the pair of anomalous cyclone and anticyclone, anomalous northeasterly winds prevail from the Yangtze River valley to BOB by the southeast of the Tibetan Plateau, implying the southwesterly winds in climatology decrease. In the composite difference of the water vapor flux (Fig. 6a), the WVT weakens from BOB to the Yangtze River valley by the southeast of Tibetan Plateau. And the WVT from SCS to East Asia increases. The contrastive relation of the WVTs from BOB and WNP to East Asia is consistent with the study from Zhang (2001).

The composite difference of 850 hPa geopotential height between the high and low WB years is shown in Fig. 4b. The East Asian continent and the western North Pacific are covered by positive values, indicating the weakened Asian low and the intensified WPSH. In 850 hPa horizontal winds (Fig. 5b), the anomalous easterly and southeasterly winds prevail over the south of the WPSH, indicating the easterly and southeasterly winds in climatology increase. The anomalous northeasterly and easterly winds prevail from East Asia to BOB by Indo-China Peninsula, indicating the westerly and southwesterly winds in climatology decrease in these regions. In the corresponding moisture flux (Fig. 6b), there exists the anomalous westward WVT in the western North Pacific and anomalous southwestward and westward WVT from East Asia to BOB by Indo-China Peninsula, implying the WVT from the south and southwest of WPSH to East Asia in climatology increases and the WVT from BOB to East Asia by Indo-China Peninsula decreases.

The 850 hPa geopotential height (Fig. 4c), horizontal wind (Fig. 5c) and the moisture flux (Fig. 6c) composites based on the WS years are similar with those based on the WB years. The Asian Low weakens and the WPSH strengthens. The anomalous easterly winds prevail over the south of the WPSH, implying the WVT from WNP to East Asia strengthens. The anomalous northeasterly winds over SCS are above the 95 % confidence level, indicating the WVT from SCS to East Asia weakens.

In general, high (low) SB may reflect the contrastive feature of the strong (weak) WVT from SCS and the weak (strong) WVT from BOB to East Asia. High (low) WB may reflect the contrastive feature of the strong (weak) WVT from WNP and the weak (strong) WVT from BOB to East Asia. High (low) WS may reflect the contrastive feature of the strong (weak) WVT from WNP and weak (strong) WVT from SCS to East Asia.

The WPSH is important for the atmospheric circulation and WVT in East Asia. Therefore, the relation of the WPSH with RIWVTPs is analyzed in this study. Figure 7 shows the WPSH positions for the high and low SB, WB and WS years, respectively. The WPSH positions are indicated with 5870 gpm in 500 hPa. There is only slight difference in WPSH positions between high and low SB years. The WPSH locates eastwards and

Discussion Paper | Discussion Paper | Discussion Paper | Discussion Paper |

CPD

9, 4263–4291, 2013

Proof in climatology for circulation effect of stalagmite δ^{18}O in East Asia

S. Nan et al.

shrink in low WB years than in high WB years. The west side is at about 140° E for low WB years and at about 120° E for high WB years. The westward and strengthened WPSH may lead more WVT from WNP to Asian continent, in favor of heavier $\delta^{18}O_s$ in East Asia in light of circulation effect; and vice versa. The WPSH positions and intensities for high and low WS years are similar with those for high and low WB years. The WPSH mainly affects the WVT from WNP to East Asia. Therefore, there exist close relations of the WPSH with WB and WS. Gong and He (2002) pointed out that the WPSH shows a significant decadal shift in the late of 1970s and the WPSH has enlarged, intensified, and shifted southwestward from 1980. It is also in agreement with the decadal changes of IWNP, WB and WS and the $\delta^{18}O_s$ in East Asia.

5 SST signal

Oceans are atmospheric moisture sources. SST in some crucial regions may affect locally and remotely atmospheric circulations, and further WVT paths and intensities. Because of slow and persistent features of ocean motion, previous signal of atmospheric circulation anomaly often can be found in oceans. Tan (2013) reveals that the El Niño-Southern Oscillation (ENSO) cycle appears to be the dominant control on the inter-annual variation in precipitation and also stalagmite $\delta^{18}O$ in East Asia. Then, are there relations of RIWVTPs with previous SST? Figure 8 shows the correlation maps of summer SB with previous and simultaneous SST. There is only small area positive correlation at the coasts of East Asia. No significant correlation is found in the equatorial central and eastern Pacific and the tropical Indian Ocean. Figure 9 is the correlation maps of WB with SST. The positive correlations appear over the equatorial central and eastern Pacific, the tropical Indian Ocean, BOB and SCS from previous autumn to this summer. The negative correlations appear over the middle latitudes in North Pacific, strengthening from previous autumn to this spring and weakening in summer. These mean that summer high WB values are associated with the El Niño phase in the equatorial central and eastern Pacific, high SST in the tropical Indian Ocean, BOB and

Discussion Paper | Discussion Paper | Discussion Paper | Discussion Paper |

CPD
9, 4263–4291, 2013

SCS, and low SST at middle latitudes in North Pacific in previous autumn and winter. The correlation maps of WS with SST (Figure is not shown) are similar with Fig. 9. In general, there are previous SST signals in the equatorial central and eastern Pacific, the tropical Indian Ocean, BOB, SCS and middle latitudes in North Pacific ahead anomalous WB and WS, and no obvious SST signal appears ahead anomalous SB.

Table 2 is the correlation coefficients of summer RIWVPs and previous and simultaneous SST in Niño3 region (5° N–5° S; 150–90° W). In agreement with Figs. 8–9, the positive correlations of the summer WB and WS with SST in Niño3 region in previous autumn and winter and this spring are above 95 % confidence level. The El Niño (La Niña) phases are associated with high (low) WB and WS. Figure 10 shows the time series of winter SST in Niño3 region for 1947/48–2010/11. SST in Niño3 region in 1976–1995 is higher than that in 1950–1975. More El Niño events occur after the midterm of the 1970s. It is in accord with higher WB in 1976–1995 than 1950–1975 in Sect. 3.3.

In the light of the circulation effect of stalagmite δ^{18}O (Tan, 2009, 2013), higher WB implies higher stalagmite δ^{18}O in East Asia. Above, it is indicated that the decadal of WB from 1950–1975 to 1976–1995 is associated with the decadal of the WPSH. Moreover, the decadal change of the WPSH in the late 1970s is closely related with winter-spring SST in the equatorial central and eastern Pacific (Gong and He, 2002). Therefore, the decadal shift of SST in equatorial Pacific is associated with the decadal shift of the WPSH, WB, and the $\delta^{18}O_s$ in East Asia.

6 Conclusions and discussions

The relative intensities of the water vapor transports (WVTs) from the western North Pacific (WNP), South China Sea (SCS) and Bay of Bengal (BOB) to East Asia are examined to verify the role of the circulation effect in decadal shift of stalagmite δ^{18}O in East Asia from 1950–1975 to 1976–1995.

In this study, the modes of moisture flux vectors are used to represent the intensities of WVT passageways. The intensities of WVT passageway from WNP, SCS and BOB to

East Asia (IWNP, ISCS and IBOB) are defined as the regionally-averaged moisture flux vector mode in the WNP (125–150° E; 10–22.5° N), SCS (107.5–120° E; 10–22.5° N) and BOB (85–100° E; 10–22.5° N), respectively. The WVT from BOB is the strongest. And the WVT from SCS is slightly stronger than that from WNP. IBOB is closely related with ISCS. They all show obvious interannual variability. The decadal shift occurs in IWNP from 1950–1975 to 1976–1995.

In light of the conception of circulation effect, the stalagmite δ^{18}O value in East Asia is mainly controlled by the relative portion variation of the local and remote WVTs. Therefore, the ratios among IWNP, ISCS and IBOB are calculated to represent the relative intensity among the WVTs from WNP, SCS and BOB to East Asia. SB is the ISCS to IBOB ratio, WB is the IWNP to IBOB ratio, and WS is the IWNP to ISCS ratio. SB, WB and WS all show the apparent interannual variations. The decadal increase occurs in time series of WB and WS, with higher values in 1976–1995 and lower values in 1950–1975, probably resulting from the strengthening of the WVT from WNP.

The atmospheric circulations and WVTs associated with SB, WB and WS are examined. In high SB years, the Asian Low and the WPSH weaken. The southwesterly winds from BOB to the Yangtze River valley by the southeast of the Tibetan Plateau weaken and the WVT from BOB to East Asia weakens. The southwesterly winds from SCS strengthen and the WVT from SCS to East Asia strengthens. In high WB years, the Asian Low weakens and the WPSH shifts westwards, enhances and enlarges. The WVT from WNP to East Asia increases because of the strengthening of the easterly winds on the south of the WPSH. The westerly and southwesterly winds from BOB to East Asia by Indo-China Peninsula decrease and the WVT from BOB to East Asia weakens. The atmospheric circulations and the WVTs associated with WS are similar with those associated with WB. For high WS years, the WVT from WNP to East Asia strengthens. The WVT from SCS weakens, above the 95 % confidence level.

There is no obvious signal in the equatorial central and eastern Pacific and tropical Indian Ocean ahead anomalous SB. WB and WS are closely related to previous SST. When the equatorial central and eastern Pacific is in El Niño phase, SST in the tropical

CPD
9, 4263–4291, 2013

Indian Ocean, BOB and SCS is high and SST at middle latitudes in North Pacific is low, WB and WS tend to be high. Previous studies indicate that the WPSH is an important circulation system influencing climate and weather in East Asia and closely related to SST in the equatorial central and eastern Pacific and tropical Indian Ocean (Wang et al., 2000; Lau and Nath, 2009; Yang et al., 2007; Xie et al., 2009). Moreover, WB and WS are closely related with the position and intensity of the WPSH. When WB and WS are high, the WPSH shifts westwards, enhances and enlarges. Therefore, SST in the equatorial central and eastern Pacific and the tropical Indian Ocean may relate to WB and WS through the WPSH.

During 1976–1995, the El Niño frequency increases. It is associated with higher WB in 1976–1995 than that in 1950–1975. In light of circulation effect of stalagmite δ^{18}O in East Asia, high WB responds for heavier stalagmite δ^{18}O. It further verifies the circulation effect of stalagmite δ^{18}O in East Asia.

Supplementary material related to this article is available online at: http://www.clim-past-discuss.net/9/4263/2013/cpd-9-4263-2013-supplement.pdf.

Acknowledgements. We thank the Climate Diagnostic Center/NOAA for providing the NCEP/NCAR reanalysis data and the Hadley Centre, Met Office for providing monthly mean HadISST data on its homepage. This work was jointly sponsored the National Natural Science Foundation of China (41030103, 41205057) and Basic Research Operation Foundation of Chinese Academy of Meteorological Sciences (2010Z003, 2013Z004).

References

Cheng, H., Edwards, R. L., Broecker, W. S., Denton, G. H., Kong, X., Wang, Y., Zhang, R., and Wang, X.: Ice Age terminations, Science, 326, 248–252, 2009.

Clemens, S. C., Prell, W. L., and Sun, Y.: Orbital-scale timing and mechanisms driving Late Pleistocene Indo–Asian summer monsoons: reinterpreting cave speleothem $\delta^{18}O$, Paleoceanography, 25, PA4207, doi:10.1029/2010PA001926, 2010.

Dayem, K. E., Molnar, P., Battisti, D. S., and Roe, G. H.: Lessons learned from oxygen isotopes in modern precipitation applied to interpretation of speleothem records of paleoclimate from eastern Asia, Earth Planet. Sc. Lett., 295, 219–230, 2010.

Gong, D. and He, X.: Interdecadal change in western Pacific subtropical high and climatic effects, Acta Geogra Phica Sinica, 57, 185–193, 2002.

Jiang, X. and Li, Y.: The review of water vapor transportation and its effects on drought and flood over China, Scientia Meteorologica Sinica, 29, 138–142, 2009.

Kalnay, E., Kanamitsu, M., Kistler, R., Collins, W., Deaven, D., Gandin, L., Iredell, M., Saha, S., White, G., Woollen, J., Zhu, Y., Chelliah, M., Ebisuzaki, W., Higgins, W., Janowiak, J., Mo, K. C., Ropelewski, C., Wang, J., Leetmaa, A., Reynolds, R., Roy, J., and Dennis, J.: The NCEP/NCAR 40-year reanalysis project, B. Am. Meteorol. Soc., 77, 437–471, 1996.

Lau, K. M. and Li, M. S.: The monsoon of East Asia and its global associations – a survey, B. Am. Meteorol. Soc., 65, 114–125, 1984.

Lau, N. C. and Nath, M. J.: A model investigation of the role of air–sea interaction in the climatological evolution and ENSO-related variability of the Summer Monsoon over the South China Sea and Western North Pacific, J. Climate, 22, 4771–4792, 2009.

Lee, J. E., Risi, C., Fung, I., Worden, J., Scheepmaker, R. A., Lintner, B., and Frankenberg, C.: Asian monsoon hydrometeorology from TES and SCIAMACHY water vapor isotope measurements 20 and LMDZ simulations: implications for speleothem climate record interpretation, J. Geophys. Res., 117, D15112, doi:10.1029/2011JD017133, 2012.

Maher, B. A.: Holocene variability of the East Asian summer monsoon from Chinese cave records: a re-assessment, Holocene, 18, 861–866, 2008.

Maher, B. A. and Thompson, R.: Oxygen isotopes from Chinese caves: records not of monsoon rainfall but of circulation regime, J. Quaternary Sci., 27, 615–624, 2012.

Pausata, F. S. R., Battisti, D. S., Nisancioglu, K. H., and Bitz, C. M.: Chinese stalagmite δ^{18}O controlled by changes in the Indian monsoon during a simulated Heinrich event, Nat. Geosci., 4, 474–480, 2011.

Rayner, N. A., Parker, D. E., Horton, E. B., Folland, C. K., Alexander, L. V., Rowell, D. P., Kent, E. C., and Kaplan, A.: A global analyses of sea surface temperature, sea ice, and night marine air temperature since the late nineteenth century, J. Geophys. Res., 108, 4407, doi:10.1029/2002JD002670, 2003.

Simmonds, I., Bi, D., and Hope, P.: Atmospheric water vapor flux and its association with rainfall over China in summer, J. Climate, 12, 1353–1367, 1999.

Tan, M.: Circulation effect: climatic significant of the short term variability of the oxygen isotopes in stalagmites from monsoonal China – dialogue between paleoclimate records and modern climate research, Quaternary Sciences, 29, 851–862, 2009.

Tan, M.: Circulation effect: response of precipitation δ^{18}O to the ENSO cycle in monsoon regions of China, Clim. Dynam., doi:10.1007/s00382-013-1732-x, in press, 2013.

Tao, S. Y. and Chen, L. X.: A review of recent research on the East Asian summer monsoon in China, in: Review of Monsoon Meteorology, edited by: Chang, C. P. and Krishnamurti, T. N., Oxford Univ. Press, New York, 60–92, 1987.

Tian, H., Guo, P., and Lu, W.: Features of water vapor transfer by summer monsoon and their relations to rainfall anomalies over China, Journal of Nanjing Institute of Meteorology, 25, 496–502, 2002.

Tian, H., Guo, P., and Lu, W.: Characteristic of vapor inflow corridors related to summer rainfall in China and impact factors, J. Trop. Meteorol., 20, 401–408, 2004.

Wang, B., Wu, R., and Fu, X.: Pacific–East Asian teleconnection: how does ENSO affect East Asian climate?, J. Climate, 13, 1517–1536, 2000.

Wang, Y., Cheng, H., Edwards, R. L., An, Z., Wu, J., Shen, C., and Dorale, J. A.: High-resolution absolute-dated Late Pleistocene monsoon record from Hulu Cave, China, Science, 294, 2345–2348, 2001.

Wang, Y., Cheng, H., Edwards, R. L., Kong, X., Shao, X., Chen, S., Wu, J., Jiang, X., Wang, X., and An, Z.: Millennial-and orbital-scale changes in the East Asian monsoon over the past 224,000 years, Nature, 45, 1090–1093, 2008.

Xie, A., Mao, J., Song, Y., and Ye, Q.: Climatological characteristics moisture transport over Yangtze River Basin, J. Appl. Meteorol. Sci., 13, 67–77, 2002.

CPD
9, 4263–4291, 2013

Xie, S. P., Hu, K., Hafner, J., Tokinaga, H., Du, Y., Huang, G., and Sampe, T., Indian Ocean capacitor effect on Indo–western Pacific climate during the summer following El Niño, J. Climate, 22, 730–747, 2009.

Yang, J., Liu, Q., Xie, S. P., Liu, Z., and Wu, L.: Impact of the Indian Ocean SST basin mode on the Asian summer monsoon, Geophys. Res. Lett., 34, L02708, doi:10.1029/2006GL028571, 2007.

Yuan, D., Cheng, H., Edwards, R. L., Dykoski, C. A., Keelly, M. J., Zhang, M., Qing, J., Lin, Y., Wang, Y., Wu, J., Dorale, J. A., An, Z., and Cai, Y.: Timing, duration, and transitions of the last interglacial Asian Monsoon, Science, 304, 575–578, 2004.

Zhang, R.: Relations of water vapor transport from Indian monsoon with that over East Asia and the summer rainfall in China, Adv. Atmos. Sci., 18, 1005–1017, 2001.

Zhou, T.: Comparison of the global air–sea freshwater exchange evaluated from independent data sets, Prog. Natural Sci., 13, 626–631, 2003.

Zhou, T. and Yu, R.: Atmospheric water vapor transport associated with typical anomalous summer rainfall patterns in China, J. Geophys. Res., 110, D08104, doi:10.1029/2004JD005413, 2005.

Zhuo, D., Zheng, Y., Li, W., and Li, X.: The disquisition of atmospheric water vapor transports and income and expenses in the typical drought and flood summer in the Jiang Huai valley, Scient. Meteorol. Sin., 26, 244–251, 2006.

CPD

9, 4263–4291, 2013

Proof in climatology for circulation effect of stalagmite δ^{18}O in East Asia

S. Nan et al.

Title Page

Abstract | Introduction

Conclusions | References

Tables | Figures

◂◂ | ▸▸

◂ | ▸

Back | Close

Full Screen / Esc

Printer-friendly Version

Interactive Discussion

Table 1. Mean and standard deviation of IBOB, ISCS and IWNP from during 1948–2011. Unit is $100\,g\,cm^{-1}\,hPa^{-1}\,s^{-1}$.

	IBOB	ISCS	IWNP
Mean	34.0	22.5	17.6
Standard deviation	3.9	3.3	2.2

CPD
9, 4263–4291, 2013

Table 2. Correlation coefficients between summer RIWVPs and previous and simultaneous SST in Niño3 region.

	Previous Autumn	Previous Winter	Spring	Summer
SB	0.07	0.03	0.10	0.07
WB	*0.35*	*0.42*	*0.36*	0.01
WS	*0.28*	*0.36*	*0.29*	−0.02

The italic is above the 95 % confidence level.

CPD
9, 4263–4291, 2013

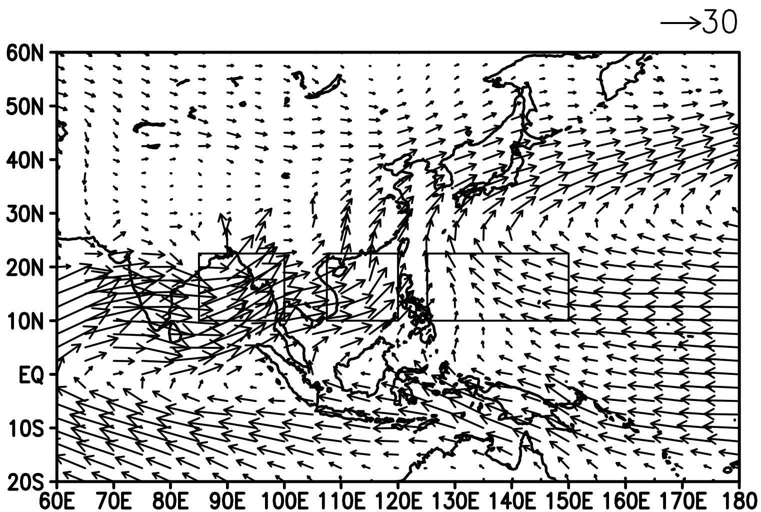

Fig. 1. The climatological mean of summer (June-July-August) water vapor flux vectors vertically integrated from surface to 300 mb during 1948–2011 (unit: $10^2\,\mathrm{g\,cm^{-1}\,hPa^{-1}\,s^{-1}}$), the three rectangles indicate the ranges of Bay of Bengal (BOB), South China Sea (SCS) and western North Pacific (WNP) from left to right successively.

CPD
9, 4263–4291, 2013

Proof in climatology for circulation effect of stalagmite δ^{18}O in East Asia

S. Nan et al.

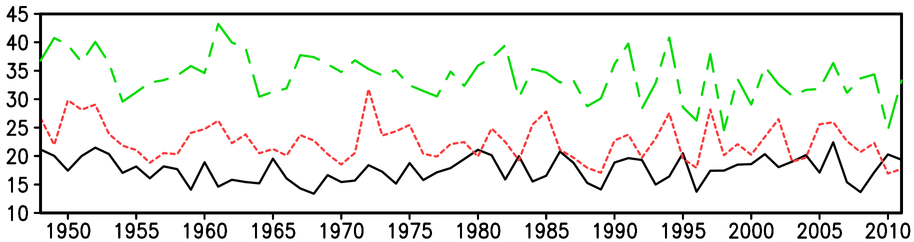

Fig. 2. Time series of IWNP (solid line; black), ISCS (short dotted line; red) and IBOB (long dotted line; green) during 1948–2011. Units are $10^2\,\mathrm{g\,cm^{-1}\,hPa^{-1}\,s^{-1}}$.

CPD
9, 4263–4291, 2013

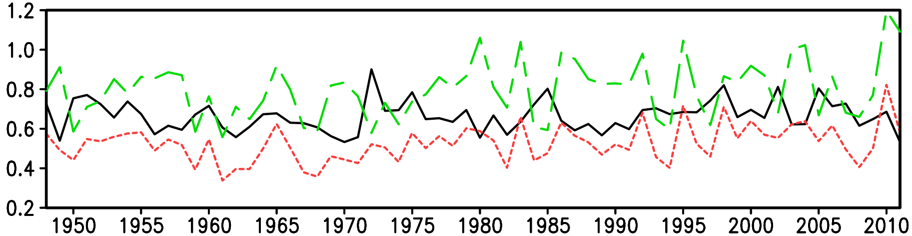

Fig. 3. Time Series of SB (solid line; black), WB (short dotted line; red) and WS (long dotted line; green) during 1948–2011.

CPD
9, 4263–4291, 2013

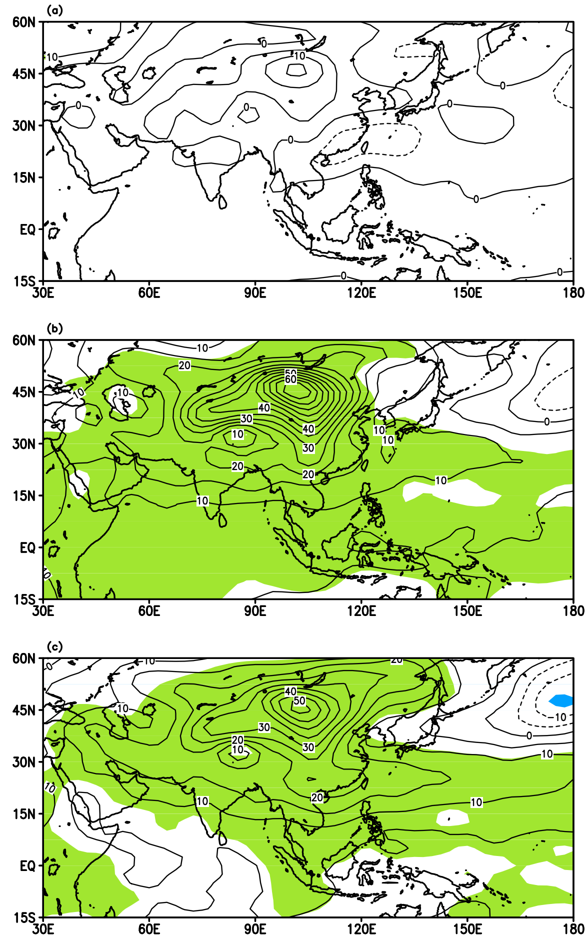

Fig. 4. Composite differences of summer 850 hPa geopotential height (m) between high and low SB **(a)**, WB **(b)** and WS **(c)**. The shaded is above the 95 % confidence level.

CPD
9, 4263–4291, 2013

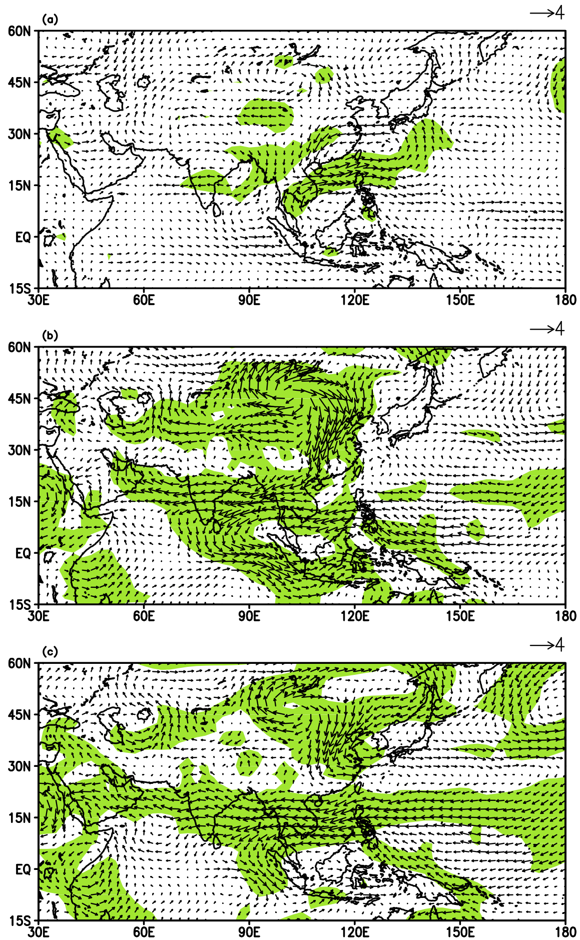

Fig. 5. Same as Fig. 4, but for the 850 hPa horizontal wind vectors (m s^{-1}). The wind vectors above 95 % confidence level are shaded.

CPD
9, 4263–4291, 2013

Proof in climatology for circulation effect of stalagmite δ^{18}O in East Asia

S. Nan et al.

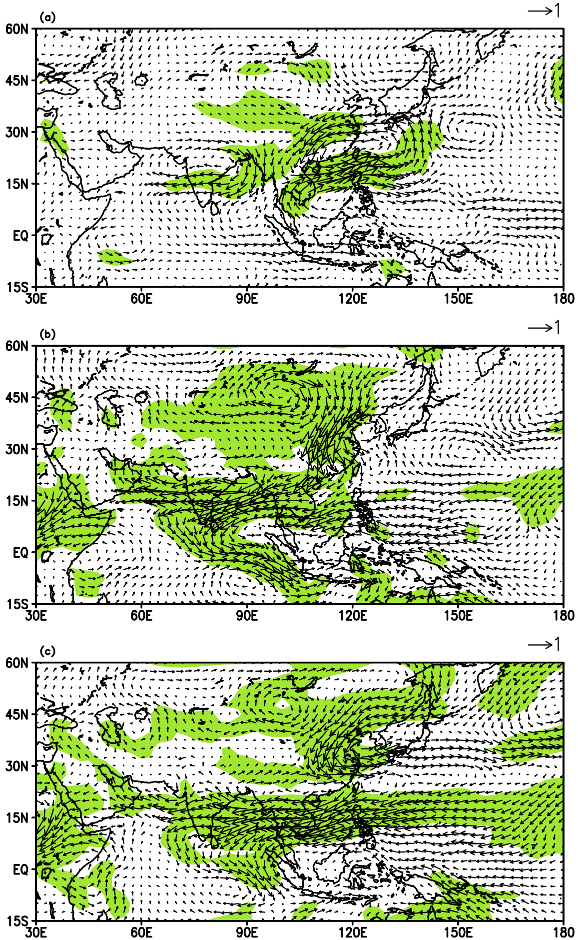

Fig. 6. Same as Fig. 4, but for moisture flux vectors vertically integrated form surface to 300 hPa (10^3 g cm^{-1} hPa^{-1} s^{-1}).

CPD
9, 4263–4291, 2013

Proof in climatology for circulation effect of stalagmite δ^{18}O in East Asia

S. Nan et al.

Title Page
Abstract | Introduction
Conclusions | References
Tables | Figures
◀I | ▶I
◀ | ▶
Back | Close
Full Screen / Esc
Printer-friendly Version
Interactive Discussion

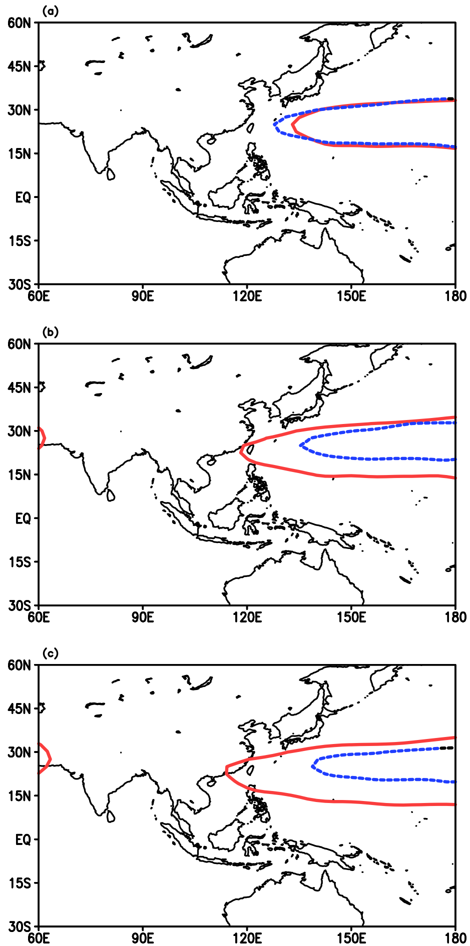

Fig. 7. Composite lines of summer 5870 gpm in 500 hPa for high (solid line) and low (short dotted line) SB **(a)**, WB **(b)** and WS **(c)**.

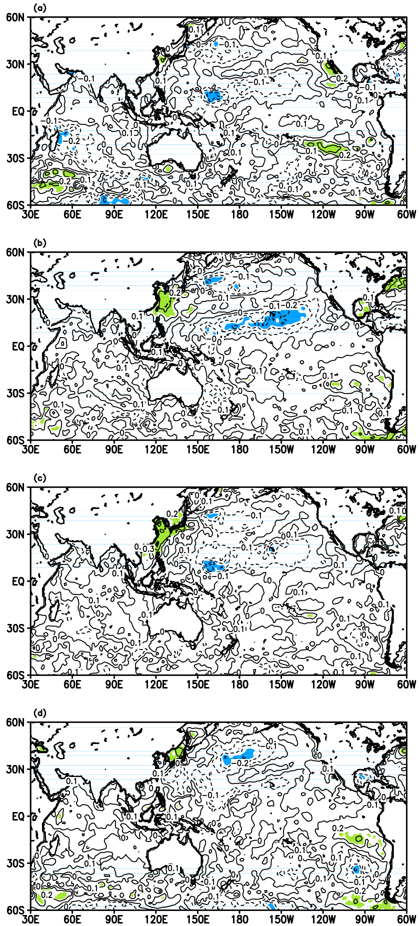

Fig. 8. Correlation maps of summer SB with SST in last autumn (September-October-November) **(a)**, last winter (December-January-February) **(b)**, this spring (March-April-may) **(c)** and summer **(d)**. The shaded is above the 95 % confidence level.

CPD
9, 4263–4291, 2013

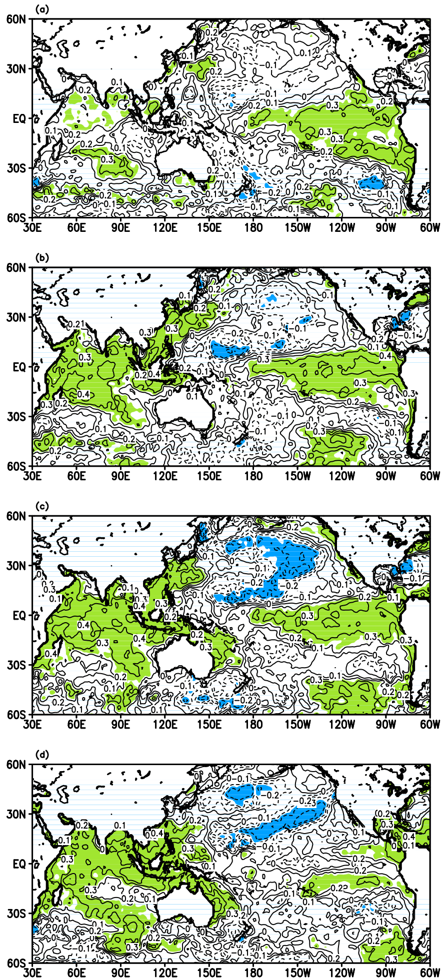

Fig. 9. Same as Fig. 8, but for the correlation maps between WB and SST.

CPD

9, 4263–4291, 2013

Proof in climatology for circulation effect of stalagmite δ^{18}O in East Asia

S. Nan et al.

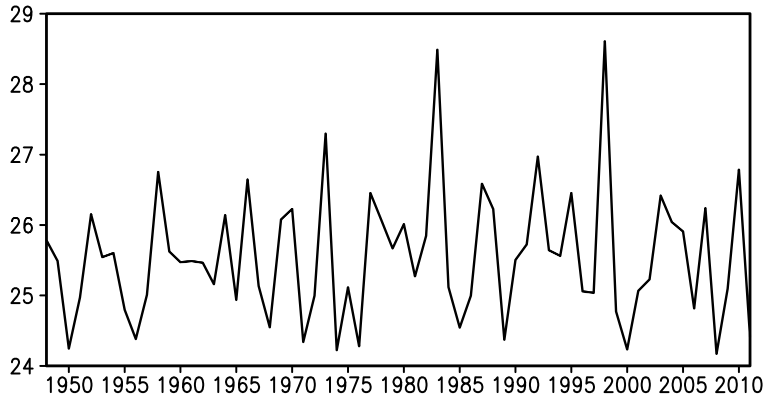

Fig. 10. Time series of SST (°C) in Niño3 region for the period of 1948–2011.

CPD
9, 4263–4291, 2013

Proof in climatology for circulation effect of stalagmite δ^{18}O in East Asia

S. Nan et al.